Greenhouse Gases: Science and Technology

ORIGINAL RESEARCH ARTICLE

Impact of Diverse Parameters on CO_2 Adsorption in CO_2 Sequestration: Utilizing a Novel Triaxial Testing Apparatus

Emad Ansari Ardehjani[1] | Mohammad Ataei[1] | Farhang Sereshki[1] | Ali Mirzaghorbanali[2] | Naj Aziz[3]

[1]Faculty of Mining, Petroleum and Geophysics Shahrood University of Technology, Shahrood, Iran | [2]School of Engineering, University of Southern Queensland, Toowoomba, Queensland, Australia | [3]School of Civil, Mining & Environmental Engineering, Faculty of Engineering and Information Sciences, University of Wollongong, Wollongong, New South Wales, Australia

Correspondence: Emad Ansari Ardehjani (eaa.emad14@gmail.com)

Received: 23 August 2024 | **Revised:** 22 December 2024 | **Accepted:** 2 January 2025

Funding: Shahrood University of Technology has sponsored and supported this research.

Keywords: CO_2 sequestration | coal | enhanced coal bed methane (ECBM) | gas adsorption | gas emission

ABSTRACT

In order to minimize greenhouse gas emissions, it is essential from an environmental point of view to employ CO_2 sequestration technology to store CO_2 in underground coal layers. To study this strategy, a triaxial testing apparatus is required. This study introduces a novel triaxial testing apparatus developed to explore enhanced coal bed methane (ECBM) and carbon dioxide (CO_2) sequestration techniques. Several laboratory tests were conducted to validate the apparatus and study the behavior of coal exposed to CO_2 using this machine. In fact, the implementation of this machine marks the initial step in an empirical feasibility analysis of CO_2 sequestration in Iranian coal seams. This analysis involves examining the impact of ash content, ambient temperature, and saturation direction on CO_2 adsorption and emission in various coal samples. Two different thermal coal samples from Chamestan and Tash mines were utilized. Some results, such as the trend of the coal sample's strain, show good correlation with previous work. Additionally, some results presented in this work are novel. On the basis of the results, the developed apparatus demonstrated satisfactory performance, and its innovative design fully meets the desired outcome. Higher ash content increases coal strength and reduces deformation. Lower ash content leads to more gas adsorption and deformation post-saturation. Gas adsorption is higher at 25°C than at 4°C. Moreover, coal samples at 25°C had 12.5 times more axial strain than those at 4°C. Lateral saturation causes 13.72% larger axial strain changes than top and end saturation due to increased gas-sample contact and penetration into the coal matrix.

1 | Introduction

Numerous studies have been carried out on the drainage of coal gas and its utilization. These studies have led to the development of coal bed methane (CBM) methods, which in turn have led to the innovation and expansion of enhanced CBM (ECBM) techniques. With the ECBM method, gas production or gas extraction from coal seams is increased by up to 95% by injecting a gaseous or liquid fluid. Most of the coal seam gas is collected for industrial and environmental applications [1]. By developing this method, the feasibility of gas recovery by CO_2[1] injection was investigated, which laid the foundation for the invention of the CO_2 sequestration method in unmineable strata or abandoned coal mines [2]. In order to use these methods to minimize and control greenhouse gas emissions, the first step is to study coal behavior.

Researchers engaged in the study and development of these methods discovered that the main engineering properties of coal, such

as uniaxial strength, modulus of elasticity, Poisson's ratio, axial and lateral strain, bulk modulus, and permeability, would change. They are altered and attenuated by the adsorption and emission of high internal energy gases such as CO_2 and CH_4.[2] Studies have shown that the extent of changes in coal's engineering properties depends on various factors, including formation conditions, coal rank, the specific coal region under study, and test conditions. Therefore, it is not possible to determine a specific pattern for the reduction of the engineering properties of coals from different regions of the world, and so for each region they must be studied individually [3–5]. However, the general behavior of coal exposed to the gases in all regions is similar. To understand this matter further, some of related works in this field are listed below.

The coal swells and shrinks due to the adsorption and desorption of gas. During adsorption, the original volume of the coal changes, and the coal undergoes linear and volumetric expansions. Linear strain refers to changes in length relative to the original sample length, whereas volumetric strain refers to changes in volume relative to the original sample volume [6]. It is worth noting that the penetration of CO_2 into the coal matrix at high pressure causes structural changes and reorganization of the coal structure. The response of the coal to the gas penetration is a transformation into a more stable and resistant structure to further CO_2 penetration [7, 8]. Experimental data indicate that the highest swelling due to gas adsorption in the coal structure is observed in the adsorption of CO_2, followed by the adsorption of CH_4 gas, whereas the adsorption of N_2 gas by coal causes the least swelling in the coal structure, which is almost zero [9].

Scientific studies have shown that the adsorption of CO_2 by coal mechanically weakens the coal layer. This gas adsorption leads to an expansion of existing fractures and cracks in the coal and also creates new fractures and cracks in the coal matrix. As a result of this phenomenon, an increase in the permeability of the coal is observed. This increase in permeability also leads to an increased emission of the methane gas present in the coal layer [10, 11].

In 1988, Ates and Barron investigated the effect of CO_2 adsorption at saturation on the strength of coal samples under a pressure of 3.45 MPa and found that the strength of the coal samples decreased by about 14% [12]. In 2006, Ranjit and Witte investigated the effects of CO_2 adsorption on the mechanical and engineering properties of lignite. According to this study, CO_2 adsorption at saturation leads to a 13% reduction in the uniaxial compressive strength (UCS) and a 26% decrease in the modulus of elasticity (E) of lignite [13].

ECBM recovery with CO_2 sequestration (CO_2-ECBM) is a promising technique for reducing greenhouse gas emissions and improving energy recovery. However, CO_2 injection can significantly impact coal seam permeability, affecting the overall efficiency of the process. To gain a deeper understanding of CO_2 adsorption, CO_2 capture and sequestration, and ECBM, we conducted a thorough examination of recent advancements in this field. The following section highlights the most cited works on CO_2 capture processes.

Su et al. [14] have investigated the mechanisms of CO_2-induced permeability reduction and recovery in coal seams. These studies have highlighted the importance of factors, such as CO_2 proportion, reservoir gas pressure, and coal properties, in determining the extent of permeability changes. By understanding these factors, it is possible to optimize CO_2 injection strategies and maximize the benefits of CO_2-ECBM [14].

Zheng et al. [15] investigated the dynamic behavior of methane desorption and CO_2 replacement during multiple CO_2-ECBM flooding cycles. Using NMR, they observed enhanced methane recovery and CO_2 sequestration with cyclic injection. The study highlighted the impact of coal type on CO_2 sorption capacity and methane recovery efficiency, with sub-bituminous coal demonstrating higher CO_2 sequestration potential [15].

Sampath et al. [16] conducted a comprehensive review of the impact of CO_2 injection on coal reservoir properties. The study highlighted the complex interplay between CO_2 and coal, emphasizing the potential for significant alterations in coal structure, including changes in permeability and strength. The authors underscore the importance of numerical modeling to accurately predict these changes and ensure the long-term viability of CO_2 sequestration in coal reservoirs [16].

Yang et al. [17] investigated the impact of water content on CO_2-ECBM processes. Their findings indicate that water plays a crucial role in CO_2 and CH_4 adsorption and desorption within coal seams. The study highlights the complex interplay among water, coal properties, and injection conditions, emphasizing the need to consider water content when optimizing CO_2-ECBM operations [17].

Kou et al. [2] developed a methodology to estimate CO_2 storage capacity in coal seams, considering factors like gas flow, diffusion, and adsorption. Their model incorporates multiple radial hydraulic fractures and provides a semi-analytical solution for bottom-hole pressure. A case study of a Wyoming coal seam demonstrated the model's effectiveness in assessing storage capacity. Sensitivity analysis revealed that hydraulic fracture length significantly impacts CO_2 storage, whereas other parameters like skin factor and stress sensitivity have limited influence [2].

Jiang et al. [18] explored the potential of utilizing post-underground coal gasification (UCG) cavities for long-term CO_2 storage. Through a large-scale numerical simulation, they investigated the transport and fate of CO_2 within the cavity over centuries. Their findings suggest that post-UCG cavities can serve as effective CO_2 sinks, with matrix–cleat diffusion being a primary trapping mechanism. The study provides valuable insights into the long-term storage capacity of these cavities [18].

Sun et al. [19] investigated the potential of fly ash–based materials for CO_2 mineral carbonization. The study examined the impact of fly ash content, water–cement ratio, and alkali addition on CO_2 adsorption capacity. Results indicated that increasing fly ash content and water–cement ratio enhanced CO_2 adsorption, whereas excessive alkali addition had a negative effect due to accelerated hydration and consumption of calcium and magnesium ions [19].

Zhang et al. [20] developed a large-scale experimental apparatus to investigate the synergistic effects of methane recovery and CO_2

sequestration in coal seams through CO_2-ECBM. Their results demonstrated increased methane recovery but decreased CO_2 sequestration efficiency with higher injection pressures. The study introduced a displacement index to evaluate the combined efficiency of both processes and highlighted the need for dynamic pressure injection. Additionally, the authors addressed limitations of previous studies by developing a more realistic experimental setup to simulate field conditions [20].

Understanding the flow conductivity of fracture channels in rock strata is crucial for optimizing gas extraction from coal seams. Zou et al. [21] have investigated the formation and evolution of fracture channels in sandstone under cyclic loading and unloading conditions. These studies have shown that the particle size distribution of fractured sandstone significantly influences the morphology and flow conductivity of fracture channels. By analyzing the proportion of fracture channels, researchers can gain insights into the complex flow patterns within rock strata and optimize gas extraction strategies [21].

Jeong et al. [22] conducted a comprehensive review of CO_2 and CH_4 adsorption on coals and shales, highlighting the importance of understanding these processes for effective CO_2-ECBM and CO_2-ESGR operations. The study explored experimental, thermodynamic, and machine learning approaches to develop predictive models for adsorption behavior, emphasizing the need for further research to address the heterogeneity of coal and shale formations [22].

Klitzke et al. [23] investigated the potential of biochar derived from banana peels as an adsorbent for methane storage. The study focused on the kinetic parameters of methane adsorption and found that a modified pseudo-first-order model best represented the experimental data. The results indicate that the activated biochar exhibits promising adsorption capacity for methane, suggesting its potential as a lightweight and efficient adsorbent for natural gas handling [23].

Chen et al. [24] conducted a gas geochemical study in a shallow coal seam to assess long-term CO_2 storage potential. The research demonstrated the effectiveness of geochemical tracers in monitoring CO_2 migration and estimating storage capacity. The study revealed a significant potential for CO_2 storage in shallow coal seams, challenging previous estimates [24].

The increasing global demand for energy and the urgent need to address climate change have driven interest in innovative energy technologies like CO_2 sequestration and ECBM recovery. These techniques offer the dual benefit of reducing greenhouse gas emissions and extracting valuable natural gas resources. However, the complex interplay between CO_2 injection and coal seam properties requires further investigation. Understanding the impact of CO_2 adsorption on coal's mechanical properties is crucial for optimizing CO_2-ECBM operations. Advanced testing equipment, such as triaxial testing machines, are essential for simulating underground conditions and studying coal's behavior under various stress and fluid injection scenarios. By addressing critical knowledge gaps in CO_2-ECBM, including the impact of different coal types and reservoir heterogeneity, researchers can unlock the full potential of this technology as a sustainable and environmentally friendly energy solution.

Iran, as a developing nation, faces the challenge of meeting its energy needs while minimizing environmental impact. Coal, a significant resource, can contribute to energy security if exploited sustainably. CO_2 sequestration and ECBM recovery offer promising solutions. To understand the behavior of Iranian coal under these processes, researchers need advanced testing equipment like triaxial testing machines. These machines will enable the simulation of underground conditions, allowing for the study of coal's mechanical properties and its response to gas adsorption and emission. By gaining insights into these factors, researchers can optimize CO_2-ECBM strategies, leading to more sustainable energy solutions for Iran.

The study aims to explore the impact of gas adsorption and emission on Iranian coal's engineering properties, along with assessing CO_2 sequestration potential in non-mineable coal layers in Iran for the first time. Special triaxial testing machinery is required to replicate underground conditions accurately, considering factors like earth pressure, thermal gradient, and fluid injection. The authors developed the first triaxial testing device and simulator to mimic these processes, comparing its performance globally. The constructed device was validated by investigating claims on CO_2 adsorption effects on coal structure, including experiments on temperature and ash content impact, re-saturation effects, gas adsorption volume, and gas emission consequences on coal sample structures.

2 | Introduction to the Triaxial Testing Machine

Gas adsorption and emission cause coal to swell and shrink, altering its engineering properties notably. Significant reductions in coal resistance and elasticity modulus occur when adsorbing gases like CO_2 and CH_4 with high adsorption capacities, leading to the formation of new cracks and fissures in the coal matrix. Studies typically focus on evaluating CO_2 sequestration and methane gas recovery methods, often utilizing triaxial tests in non-mineable layers or abandoned mines. These tests aim to simulate deep underground conditions and assess changes in engineering properties induced by gas adsorption.

The triaxial compression test is a proven tool for laboratory investigations and experimental hydro-mechanical rock tests in geotechnics and geosciences. This tool allows the acquisition of valuable information on rock behavior and easy control of many external parameters, such as fluid injection pressure, axial stresses, and containment pressure during the experiment [25]. For a comprehensive understanding of the geomechanical processes involved in CO_2 sequestration and ECBM methods, accurate simulation of subsurface reservoir conditions in the laboratory is crucial. Key conditions for simulating these processes include high pore pressure, lateral pressures, and temperature increases to simulate geothermal gradients [26].

To date, extensive research has been conducted using triaxial tests to investigate the flow behavior of CO_2, CH_4, N_2, He, water, and brine during mechanical tests on various rock types such as sandstone, limestone, shale, and coal, and to study the behavior of fluid passage through the rock and rock resistance during this transfer [27]. However, it should be noted that the extent of these changes in the engineering properties of coal varies

depending on the type of gas, the nature and type of coal seam, the structure of fractures and inherent fractures, the depth of the coal seam, and other factors. Therefore, a more detailed study and measurement of these properties is required for each coal region [28]. Depending on the research needs, various devices and designs have been proposed and implemented by researchers; for more information, you can check these references [29].

3 | Introduction to the Various Units of the Triaxial Testing Machine

The engineering characteristics and permeability of porous rocks are investigated in situ using a triaxial testing apparatus. This device can model a range of stresses, fluid injection pressures, and predicted temperatures during CO_2 sequestration and ECBM processes. It is primarily intended for use in experimental simulations linked to these processes. The device enables constant control over fluid flow rates, lateral and axial displacements, axial and axial tensions, and the amount of injected and ejected fluids. It also permits the sample to be saturated with liquids. This device typically consists of the following five basic sections: (1) pressure cell; (2) pressure application unit; (3) heating system unit; (4) piping and fluid injection system; and (5) measurement and data collection unit.

4 | The Aim of Device Development

The primary objective of this research is to introduce a novel triaxial testing apparatus designed to investigate the behavior of coal under simulated underground conditions, with a specific focus on CO_2 sequestration and ECBM processes. This apparatus enables the controlled experimentation of various factors, including gas pressure, temperature, and saturation direction, to assess their impact on coal's mechanical properties and gas adsorption/emission characteristics. By providing valuable insights into coal's response to these processes, this research contributes to the advancement of CO_2 sequestration technologies and the optimization of ECBM operations.

5 | Manufacturing Triaxial Testing Machines in Iran

5.1 | The Idea of Designing the Pressure Cell (Hook Cell Redesign)

The pressure cell is crucial in the triaxial testing machine for studying gas effects on coal properties under different pressures. It's critical to carefully design this cell. It forms the core of the testing apparatus by integrating vital instruments, such as hydraulic pumps, load cells, heating systems, and flow meters.

One popular technique for determining the triaxial strength of rock is to apply hydraulic pressure to a sample and then subject it to axial pressure till failure. To prevent pore pressure problems, it is essential to make sure that no hydraulic fluid leaks into the sample. These issues were resolved by Hook and associates' 1968 triaxial strength measuring cell, which worked by pouring oil into the space between the cylinder and cell wall to facilitate the simple removal of samples and strain gauges. Their invention greatly decreased the cost of triaxial testing while also increasing testing simplicity and workshop convenience [30].

Although injecting and collecting fluid from the rock sample presents a substantial barrier, the Hook cell applies triaxial pressure to the material. Another problem is connecting the output of strain gauges to the outside of the cell to collect data, all the while making sure the cell is sealed against gas leaks.

Three pieces of nickel-containing alloy steel (Steel 5920)—the head, body, and chamber end—were machined to fulfill objectives inspired by the Hook cell. Steel 5920, known for its 18 CrNi8 composition, is ideal for cementation procedures due to its low carbon content and chromium presence. With nickel enhancing hardness, steel 5920 boasts a 217 Brinell (HB) hardness and finds common use in high-toughness applications like flat wheels and large gear wheels. This unique cell design allows for both axial and lateral injection of oil and gas into coal samples, providing versatility in pressure application. The subsequent sections delve into the detailed components and applications of both types of device sets.

This innovative pressure cell design enhances its capability for a range of rock and fluid mechanical tests beyond simulating ECBM and CO_2 sequestration. Figure 1 illustrates fluid injection points for gas and oil in both device sets. Figure 1a allows lateral gas circulation around the coal sample under axial pressure, suitable for studying gas effects on coal parameters and pillar stability. It simplifies axial force application by using an oil pump instead of an automatic press. Figure 1b mimics traditional triaxial test cells for modeling CO_2 sequestration and ECBM processes. It applies gas and axial pressure, whereas confining pressure is oil-applied to the sample's sides. Subsequent sections detail the pressure cell, load application unit, gas injection, thermal system, and data collection methods.

5.2 | Pressure Cell

The pressure cell components for simulating CO_2 sequestration and ECBM processes are detailed. The head of the cell includes a hollow with collar piece for axial force. An O-ring seal prevents leaks at the collar. A permeable cylinder allows gas injection above the coal sample. The head features a 1/4 in. port for gas/oil injection, a gas outlet, and connections to a flowmeter and balance. A flange secures the head to the body.

The cylindrical body holding the rock sample has thermal belt elements, ports for oil/gas collection, and gas/oil injection. A plastic membrane applies lateral pressure to the coal sample. Flanges at both ends seal the cell with O-ring seals. The end section mirrors the head in geometry and dimensions, with a cylinder supporting the coal sample. It includes inputs, outputs, and provisions for data extraction from strain gauges and sealing against fluid leaks (Figure 2).

5.3 | Pressure Application Units

The pressure unit in this device consists of two parts: axial loading and confining pressure. Each part is explained in detail in the following sections.

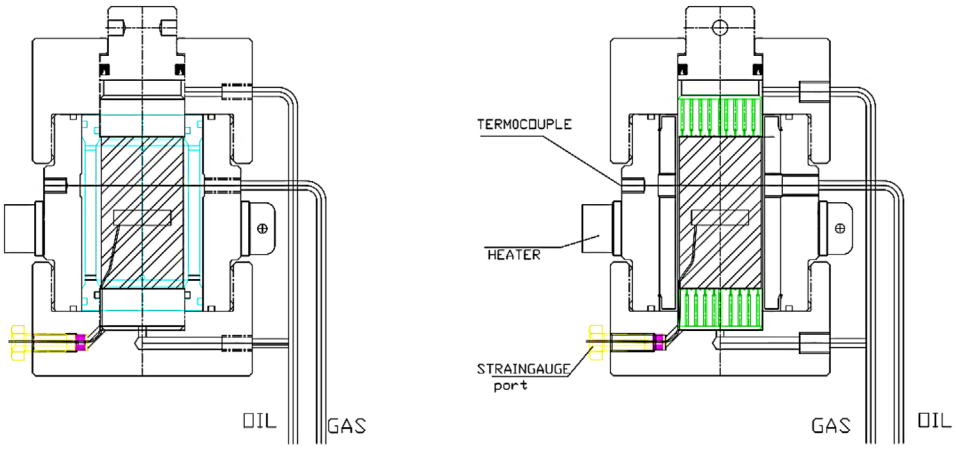

Figure 1 | Schematic view of the designed pressure cell: (a) for simulating coal pillar conditions; (b) for simulating ECBM and CO_2 sequestration processes.

5.3.1 | Axial Loading Application Unit

Two methods provide axial loading to the coal sample in this setup. First, it is placed under UCS testing equipment provided by Shahrood University of Technology. The equipment, an automated machine from Controls Italy, includes an eight-channel data logger and a hydraulic pressure jack capable of applying 3000 KN. Axial loading is applied through the collar section on the cell head. The second method utilizes an oil pump to apply axial loading on the top and bottom sides of the sample. This approach, part of an assembly examining gas emissions' impact on coal pillar stability, allows for continuous and prolonged loading on the coal sample in both scenarios (Figure 2).

5.3.2 | The Confining Pressure Application Unit

Similar to the Hoek cell, this device uses a plastic membrane to apply confining pressure on the sample (Figure 2c). Next, oil is sprayed at a precise pressure all around the sample using an oil pump. The set of simulation devices for the ECBM process (Figure 1b) must be utilized in order to deliver confining pressure to the sample. Up to 400 bar of oil pressure can be applied using the oil pump found in the rock mechanics lab.

5.4 | Piping and Fluid Injection System

Fluid injection system consists of two parts: gas cylinders (fluid reservoirs) and fluid transmission and pressure control system. Below, both sections and their components are described.

5.4.1 | Fluid Reservoirs

For studying ECBM and CO_2 sequestration processes, CH_4 and CO_2 cylinders are required. The CH_4 cylinder used in this device is a 40-L cylinder containing 99.9% pure CH_4 gas filled at a pressure of 160 bar. The CO_2 cylinder is also a 40-L cylinder with 99% purity filled at a pressure of 50 bar.

5.4.2 | Fluid Transmission and Injection System

This section features high-pressure fluid transmission pipes, a 100-bar gas regulator, one-way input valves (Ball-Valve 1/4), and pressure gauges. Gas from the cylinder is regulated by a 100-bar output gas pressure regulator before entering the pressure cell through one-way valves and high-pressure pipes rated for up to 250 bar. Pressure loss along the transmission path is minimal, eliminating the need for a pressure gauge at the gas inlet. CH_4 and CO_2 are injected at pressures ranging from 10 to 100 bar and 10 to 50 bar, respectively, without requiring a gas pressure booster due to cylinder output pressures.

5.5 | Heating System Unit

Utilizing a thermal belt with a circular heating element and thermocouple, controlled by a digital panel, mimics Earth's thermal gradient. This system can reach 60°C inside the cell within 30 min. The thermocouple in a drilled cavity and the heating element around the cell body manage temperature. Apply electrical current to activate temperature control. Ensure the thermocouple maintains contact with the device to prevent overheating.

5.6 | Measurement and Data Collecting Unit

This device measures axial and lateral displacements, strains, gas injection pressure, confining pressure, axial load, coal sample resistance, failure time, residual resistance, and internal temperature. Key measurement techniques include the following:

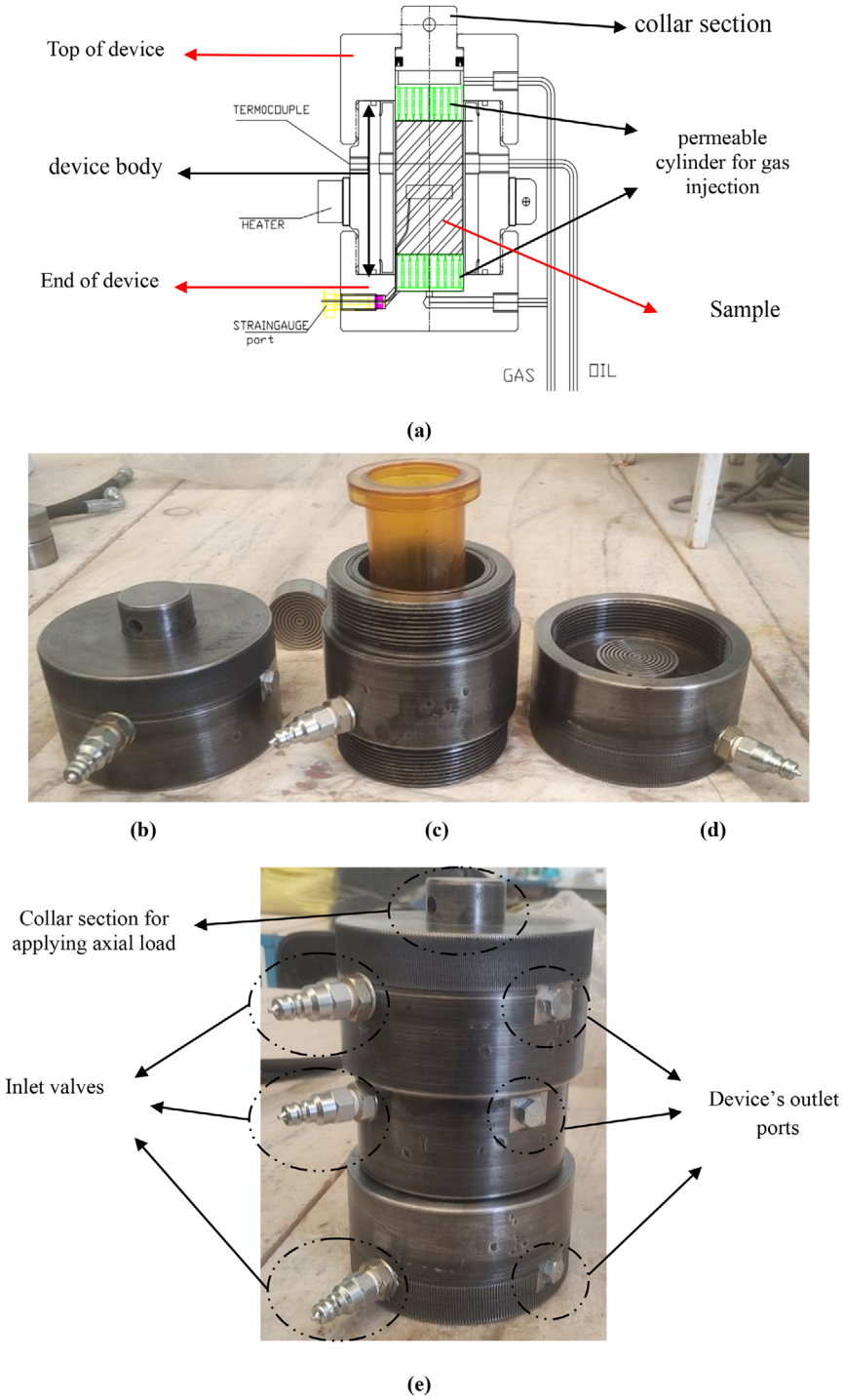

Figure 2 | (a) Schematic overview of the designed pressure cell; (b) head; (c) body; (d) end of the designed cell; (e) assembled pressure cell unit.

- Strain gauges track lateral and axial strains induced by gas processes and pressures, ensuring leak-free operations.
- Displacements are monitored using strain gauges, or vertical shifts measured by using an accurate clock on a collar piece.
- Stress–strain curves, resistances, axial loads, and gas exposure effects are automatically recorded.
- Confining pressure is gauged by a pump-mounted pressure gauge, whereas gas injection pressure is regulated at 100 bar.
- Internal temperature is monitored by a thermocouple and digital panel.
- Gas flow and output are currently unmeasured, but provisions for gauging them are in place for future development.

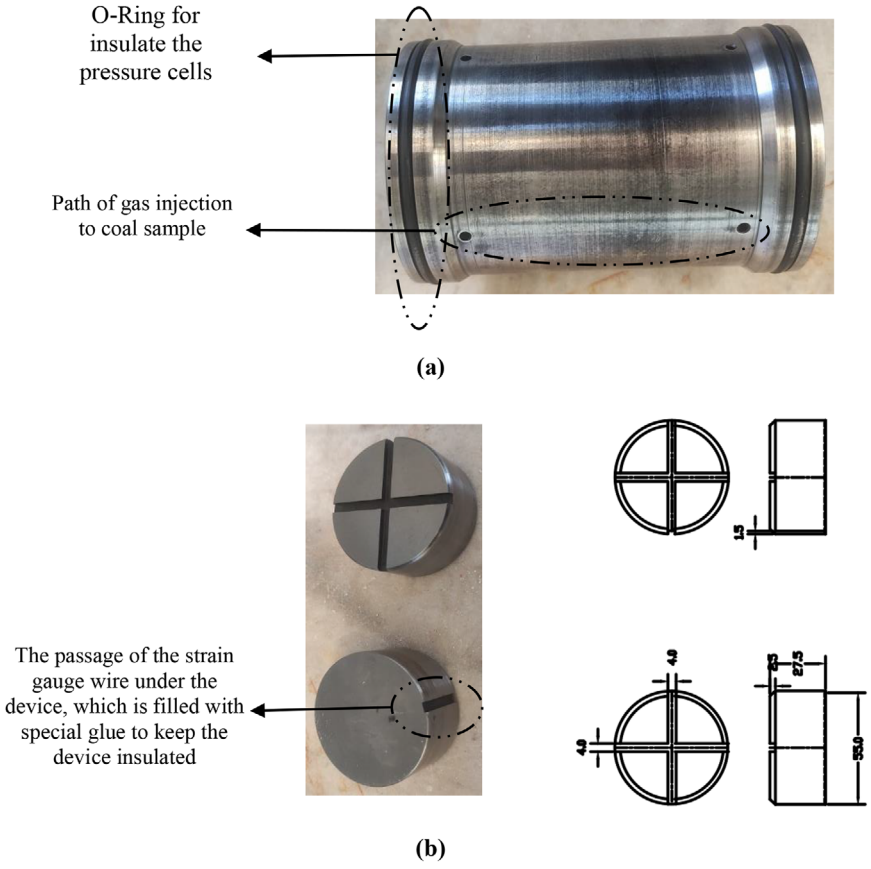

Figure 3 | (a) Permeable cylinder; (b) solid axial load transfer components.

6 | Simulation of the CO_2 Sequestration Process Using the New Triaxial Testing Machine

To simulate CO_2 sequestration effectively, an additional equipment set is necessary to circulate gas around the coal sample. The sample is enclosed in a permeable steel cylinder instead of a plastic barrier, ensuring better gas insulation. O-rings in the cylinder secure gas-tight sealing between the sample and the device. Components in the setup enable applying axial pressure using an oil pump or press. By saturating the sample with gas, researchers can analyze how gas influences coal engineering properties. This setup operates akin to an ECBM simulator, allowing for data extraction on gas effects (Figures 2 and 3).

7 | The Device Advantages

In addition to modeling the processes of CO_2 sequestration and ECBM to investigate the underground coal seams in deep mines, this flexible device may also be utilized for simpler tasks, like serving as a triaxial cell to determine the triaxial resistance of various types of rocks. This device has a very low construction cost compared to other devices that are available globally, and because of its multifunctionality, it offers more operational capabilities than other devices. In fact, three entirely different processes can be readily simulated by building one device. The device is easy to create, repair, and maintain because of its unique and strong design, which also makes it resistant to damage in any situations. The device has significantly cheaper maintenance and repair expenses than its worldwide parallels, and in the unlikely event of damage, it can be readily repaired.

8 | Triaxial Testing Machine Validation

8.1 | Sample Preparation

This research employed two samples of thermal coal from the Chamestan region in Mazandaran province and Tash village in Shahrood county, Semnan province. The Tash region is located in the middle of Iran's Alborz Mountain range, whereas the Chamestan region is located in the range's northern sections. Blocks larger than $20 \times 30 \times 30$ cm^3 were taken out of these two mines' coal seams and brought to Shahrood University of Technology's rock mechanics and rock-fluid laboratory in the Faculty of Mining, Petroleum, and Geophysics Engineering. Table 1 lists the major features of these two coal samples, such as moisture content, ash content, volatile matter, and organic matter (maceral). This table shows that the Tash coal mine has substantially less ash than the thermal coal from Chamestan. Tests for rock mechanics were conducted in accordance with ASTM standards, and cylindrical samples measuring 54 mm in diameter and 100 cm in length were taken out and separated from the coal blocks. Following their separation, the samples were stored between multiple plastic layers to guard against moisture

Figure 4 | Preparation stages of coal sample for testing.

Table 1 | Characteristic parameters of Chamestan and Tash coals.

Parameter (%)	Chamestan	Tash
Moisture content	1.7	2.4
Ash content	13	4
Volatile matter	31	32.4
Organic matter	54.3	61.2

loss and air oxygen oxidation. Figure 4 shows the stages of sample processing.

8.2 | Examination Method

In order to investigate the effects of temperature, ash content, and the direction of gas adsorption (from the sample's wall or both ends), all samples were put inside the chamber of a triaxial testing machine and exposed to CO_2 for about 72 h at a pressure of 30 bar. A strain gauge (TML 120 Ω) with a length of 30 mm attached to a data logger was used to record the axial variations of the gas-saturated sample throughout this time. The axial variations of the coal sample caused by CO_2 saturation at constant injection pressure were investigated using this strain gauge under a range of temperature settings, ash content, and saturation direction. Apart from the previously mentioned aspects, the axial alterations in the coal sample resulting from CO_2 emissions were also documented and examined. It is important to note that in this investigation, there is a notable distinction between gas emission and desorption. In the event of a gas emission, the sample is permitted to gradually release the saturated gas over time without the vacuum pump's assistance. The axial strain gauge documented the sample's axial changes in form during this time. The time it takes for the sample to get saturated with CO_2 is the same as the length of gas emission.

8.3 | Impact of Ash Content on the Mechanical Behavior of Coal and CO_2 Adsorption Capacity

Coal's adsorption capability is negatively impacted by its ash content [31, 32]. According to a study by Dutta et al., coal's adsorption capacity for CO_2 and CH_4 decreases by 2 and 0.90 mL/g, respectively, with every 1% rise in ash concentration. On the other hand, Weniger et al. [33] and Weishauptová et al. found no discernible relationship between the ash content and coal's adsorption capacity [34, 33]. Additionally, minerals adversely affect the adsorption of coal's gas contents [35–37]. According to a study by Dutta et al., a 1% increase in minerals lowers coal's adsorption ability for CO_2 by 2 mL/g and CH_4 by 1 mL/g [36]. Nonetheless, Romanov et al. claimed that the extremely porous mineral composition of Fruitland coal increases the coal's capacity for adsorption [38]. The "dilution effect" of minerals on the significance of CH_4 adsorption was reported by Weniger et al. [33, 39]. Even though they have different characteristics, ash and minerals are both inorganic coal constituents that have an impact on the coal's ability to adsorb gases. In both dry and wet situations, there is a favorable correlation between the moisture content of coal and its gas adsorption capability [36, 39]. For Indian coal, Dutta et al. showed that an average of 15% increase in organic carbon results in an increase in adsorption capacity of 15 mL/g for CH_4 and 40 mL/g for CO_2 [36].

Two thermal coal samples with varying percentages of ash were used to examine the effect of ash content on the amount of CO_2 adsorption by coal samples. Samples of thermal coals from Tash and Chamestan, with ash percentages of 4% and 13%, respectively, were used for this purpose (Table 1). Using a uniaxial compression resistance testing machine, the axial strain and UCS of both coal samples were determined in the first step. Axial strain and UCS variations were plotted before and after failure for both samples, which were subjected to a loading rate of 0.1 kN/s under a hydraulic jack.

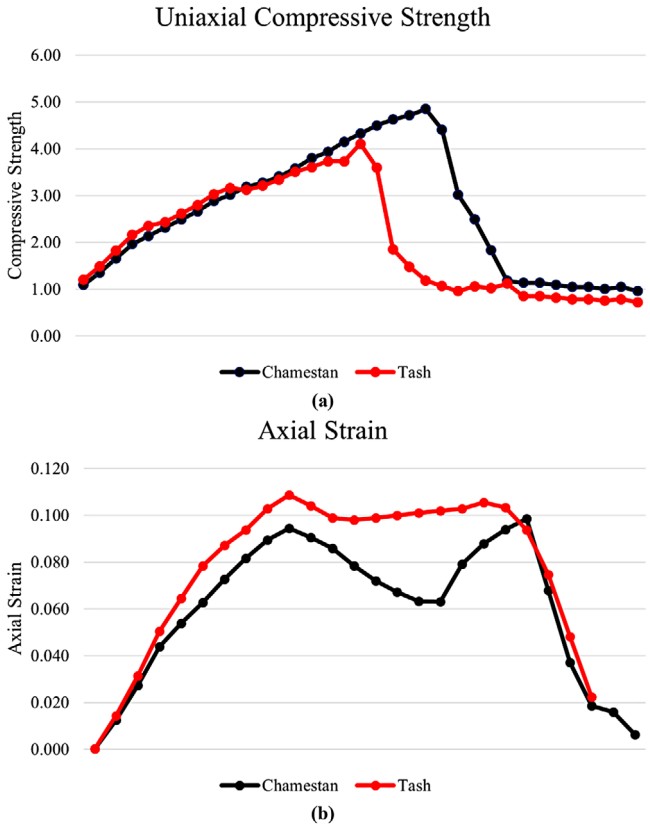

Figure 5 | (a) Comparison of the trend of uniaxial compressive strength changes; (b) comparison of the trend of axial strain changes under uniaxial pressure for Chamestan and Tash thermal coals.

Figure 5a shows that because Chamestan coal has a larger ash percentage than Tash coal, its UCS is about 17.76% higher. Prior to failure, the maximum UCSs for the coals in Chamestan and Tash were determined to be 4.85 and 4.11 MPa, respectively. The trends of variations in the two coal samples' UCSs are shown in Figure 5a.

Plotting and comparing the graphs of the axial strain changes for the two coal samples during uniaxial failure made it clear that Chamestan coal's axial strain before failure is roughly 9.17% smaller than the calculated axial strain in Tash coal because of the coal's greater ash content. For Tash and Chamestan coals, the maximum estimated axial strain was 0.109% and 0.099%, respectively (Figure 5b).

A higher amount of coal ash results in higher UCS and lower axial strain under uniaxial pressure. Basically, brittle failure behavior is more prevalent in coal with a higher ash percentage. Figure 5a shows that the samples exhibit strain-softening behavior because of a sudden drop in resistance along a plane where there hasn't been any prior significant deformation [40]. This kind of coal behavior suggests that the strain-softening behavioral model is a superior choice for numerical modeling in the design, stability, failure, and behavior prediction of coal mine walls, roofs, floors, and faces.

The two samples' dual-axial strain graphs show that there were two failures that occurred in them. The initial breakdown manifested as an unfinished fracture, and hence, the initial graph cover assumed an unfinished shape. When a fracture occurs and the fracture plane does not fully split the sample and emerge from both sides, it is referred to as an incomplete fracture. The sample continues to alter and load after being reloaded. Resistance and axial strain suddenly decrease as the second cover forms as a result of the sample failure.

For about 3600 min, or 60 h, the coal samples were exposed to CO_2 at a temperature of 25°C and an injection pressure of 30 bar from the surrounding wall (Figure 6). The data logger device recorded the coal sample's axial strain changes at a rate of three data points per second during the gas adsorption operation. Figure 7a compares the axial strain variations caused by CO_2 adsorption in the two samples. The injected gas encloses the coal sample like a confining pressure at the start of the experiment. The axial strain rises sharply in the first moment following gas entry. This sharp rise is brought on by the sample's axial shape changing as a result of both gas pressure–induced and gas adsorption–induced sample deformation. For both samples, the biggest axial strain and shape changes happened within the first hour of the adsorption phase. The axial strain changes during the first 600 min of gas adsorption are shown in Figure 7b.

These graphs show that in the Tash coal sample, gas adsorption is about 19.41% more than in the Chamestan thermal coal due to differences in axial strain. For Tash and Chamestan coals, the computed axial strain was 0.814% and 0.656%, respectively. Consequently, the coal's enhanced gas adsorption capacity and decreased ash content lead to increased strain changes in the coal. For coal samples, a saturation duration of roughly 10 h is sufficient, according to the pattern of axial strain variations. The axial strain of the coal will not significantly alter after this point due to time and gas exposure; thus, this quantity can be disregarded to speed up the testing procedure.

8.4 | The Impact of Temperature on CO_2 Adsorption

Day et al. [41] reported that swelling is inversely correlated with temperature. Raising the temperature causes the volume of gas adsorbed to decrease, which lowers the strain that adsorption causes to be produced. According to the research of Dai et al., adsorbed materials show more swelling at higher critical temperatures; in other words, the maximum swelling rises linearly with the adsorbed substance's critical temperature. They also discovered that swelling starts at a pressure of 3 MPa at lower temperatures (25°C) [42–44].

In this set of trials, the heater's elements first heated the cell to 50°C over the course of 30 min in order to obtain a temperature of 25°C. The device's display screen temperature has been lowered to 25°C following the injection of gas into the cell pressure. This avoided the sudden reductions in temperature brought on by the injection of CO_2. The Chamestan coal sample was saturated with CO_2 at two temperatures: 25°C and 4°C at an injection pressure of 30 bar for 3600 min in order to examine the impact of temperature on the amount of gas adsorption by the coal sample. Then, the amount of axial strain changes following CO_2 adsorption at these two temperatures was recorded and compared. The trend of axial

Figure 6 | Pressure cell view during the saturation of the coal sample with CO_2.

strain variations after 3600 min of CO_2 adsorption at 25°C and 4°C is shown in Figure 8.

As seen in Figure 8, the sample's axial strain initially increases by 0.2% at 4°C when gas is injected. The confinement force applied by the gas injection pressure makes these changes in axial strain more noticeable. The coal sample shrinks with time at 4°C, and its axial strain is demonstrated to be tensile and decreasing. A closer look at the axial strain change curve reveals an in steps increase in axial strain in the coal sample after gas adsorption (Figure 8b), although these strain changes may be missed because of the small size of the calculated strain.

The coal sample's axial strain at 25°C is 12.5 times higher than the computed axial strain at 4°C when looking at the presented graphs in Figure 8a and the axial strain variations. Under these interpretations, the temperature's influence on the coal sample's ability to adsorb gas is clearly visible. The results of this experiment, together with other research, indicate that 25°C is the ideal temperature for coal to adsorb gases to the greatest extent possible.

8.5 | Impact of Saturation Direction on the Coal Sample Gas Adsorption Capacity

Previous studies typically saturated coal samples from both ends due to device limitations. This study's equipment allows for saturation from both ends and the lateral walls, aiming to mimic CO_2 sequestration in unmineable coal seams and abandoned mines. Saturating the coal sample from both ends simulates conditions in deep, thin coal layers. Confining pressure replicates conditions in coal seams at depth while mimicking CO_2 sequestration in abandoned mines by saturating from the perimeter. Additionally, applying axial force can mimic vertical stress on coal pillars for underground stability analysis.

In this study section, the coal sample underwent dual saturation—once from the perimeter and once from both ends—under the same gas injection pressure and temperature for 3000 min to compare gas adsorption capacity. Axial strain changes were monitored over time during saturation, as depicted in Figure 9. Comparing axial strain changes, saturating from the perimeter resulted in approximately 13.72% higher strain than saturating from both ends. Post-saturation, axial strain values at the sample's perimeter and both ends were 0.656% and 0.555%, respectively. The larger gas contact surface during saturation from the perimeter explains this difference. Axial strain increases in a step-wise manner from both ends during saturation, creating new fissures and cracks due to increased sample volume from CO_2 exposure. This expansion allows gas to penetrate the coal structure through new pathways, resulting in swelling and further gas adsorption, leading to the formation of additional cracks and fissures with each strain increase.

8.6 | Axial Strain Variation Following Subsequent Saturation of a Coal Sample

Initially, the coal sample was saturated with CO_2 for 3200 min at 30 bar and 25°C to study its behavior during adsorption. Subsequently, the sample underwent a 3200 min natural gas release period at the same temperature. Following this, another 3200-min CO_2 saturation was conducted, as depicted in Figure 10, showing axial strain changes. The experiment revealed a 70% decrease in axial strain changes during the subsequent saturation, attributed to the lack of free surfaces for CO_2 re-adsorption in fissure walls. The full saturation of gas in the sample's body during the first saturation phase limited further adsorption, showcasing coal's robust CO_2 sequestration capability. With its porous nature, coal serves as an ideal medium for CO_2 storage and sequestration operations.

8.7 | Examining the Impact of Gas Emission on the Saturated Coal Sample Structure

In this experiment, the gradual release of gas from a saturated sample, known as "gas emissions," is studied by stopping the gas pressure under consistent temperature and time conditions after

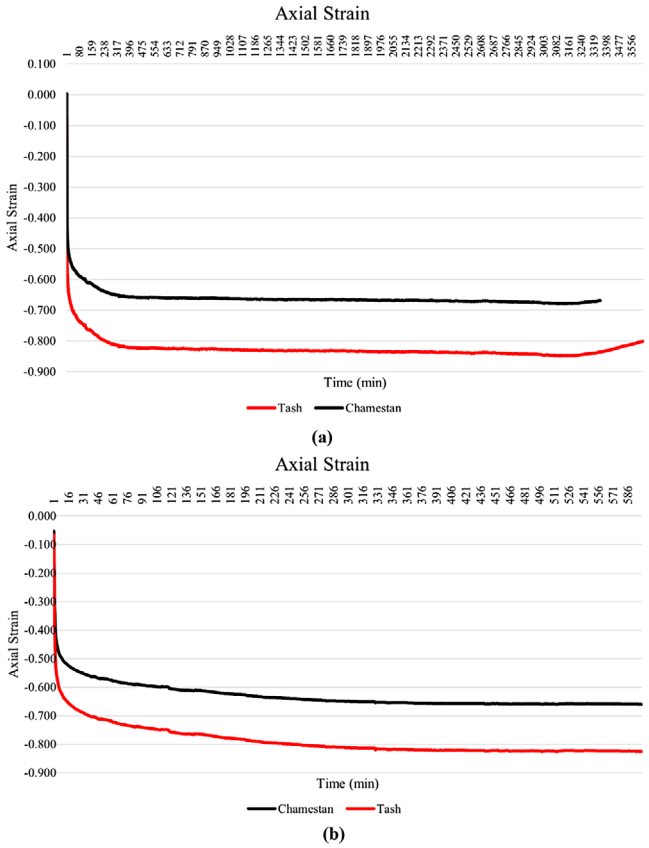

Figure 7 | (a) Comparison of axial strain changes graphs resulting from CO_2 adsorption with an injection pressure of 30 bar from the perimeter wall of Tash and Chamestan coal samples at a temperature of 25°C during 3600 min of saturation time; (b) comparison of axial strain changes graphs resulting from CO_2 adsorption with an injection pressure of 30 bar from the perimeter wall of Tash and Chamestan coal samples at a temperature of 25°C during the first 600 min of saturation time.

the saturation period. This mimics the natural gas release process from coal seams in abandoned mines during CO_2 sequestration, allowing for observation of coal pillar behavior and stability over time.

Figure 11a,b displays the axial strain changes of Chamestan and Tash coal samples after 3200 min of saturation at 30 bar and 25°C, as well as the resulting axial strain changes during 3200 min of gas emission at 25°C. The axial strain of Chamestan coal decreased from 0.656% to 0.056% post gas emission, marking a 91.46% reduction from the saturated state. Similarly, Tash coal showed a reduction from 0.814% to 0.065%, indicating a 92.02% decrease in axial strain. Despite Tash coal having lower ash content than Chamestan coal, its higher axial strain change after gas emission suggests a greater gas adsorption capacity due to its lower ash percentage.

9 | Discussion

The development and successful validation of the novel triaxial testing apparatus represent a significant advancement in the field of coal research. This apparatus enables precise control over experimental conditions and accurate measurement of key parameters, providing valuable insights into the complex interactions between coal and gas.

The experimental results obtained in this study have shed light on several key aspects of coal behavior under CO_2 sequestration and ECBM conditions. The impact of ash content on coal's mechanical properties and gas adsorption capacity was investigated. Consistent with previous studies [36, 39], our findings indicate that higher ash content generally leads to reduced gas adsorption and increased mechanical strength. However, the specific relationship between ash content and coal properties can vary depending on the coal type and mineral composition.

The effect of temperature on gas adsorption was also examined. As expected, higher temperatures resulted in lower gas adsorption, aligning with previous studies [42–44].This observation can be attributed to the reduced gas adsorption capacity at higher temperatures.

The impact of saturation direction on gas adsorption was investigated, revealing that lateral saturation resulted in higher gas adsorption compared to end and top saturation. This finding can be attributed to the increased contact area between the gas and the coal sample during lateral saturation, allowing for deeper penetration of the gas into the coal matrix.

The study also explored the potential for multiple cycles of gas adsorption and emission. The results suggest that the initial saturation cycle significantly impacts the subsequent adsorption capacity of the coal. This information is crucial for optimizing CO_2 sequestration and ECBM operations.

Although our study aligns with previous research on the general trends of gas adsorption and its impact on coal properties, it provides novel insights into the specific behavior of Iranian coal samples. The unique characteristics of Iranian coal, such as its mineralogical composition and structural properties, may influence its response to gas adsorption and desorption.

Although this study provides valuable insights, it is important to acknowledge its limitations. The number of coal samples tested was relatively small, and the experimental conditions were specific to the laboratory setup. Future studies could expand the sample number and explore a wider range of experimental conditions to obtain a more comprehensive understanding of coal behavior.

Future research could also focus on investigating the long-term effects of CO_2 sequestration on coal seam stability and the potential for induced seismicity. Additionally, advanced modeling techniques could be employed to simulate the complex processes involved in CO_2 sequestration and ECBM.

The development of the triaxial testing machine and the experimental results presented in this study contribute to a better understanding of coal's response to gas adsorption and desorption. By addressing the limitations of previous studies and providing new insights into the behavior of Iranian coal, this research has the potential to inform the optimization of CO_2 sequestration and ECBM strategies.

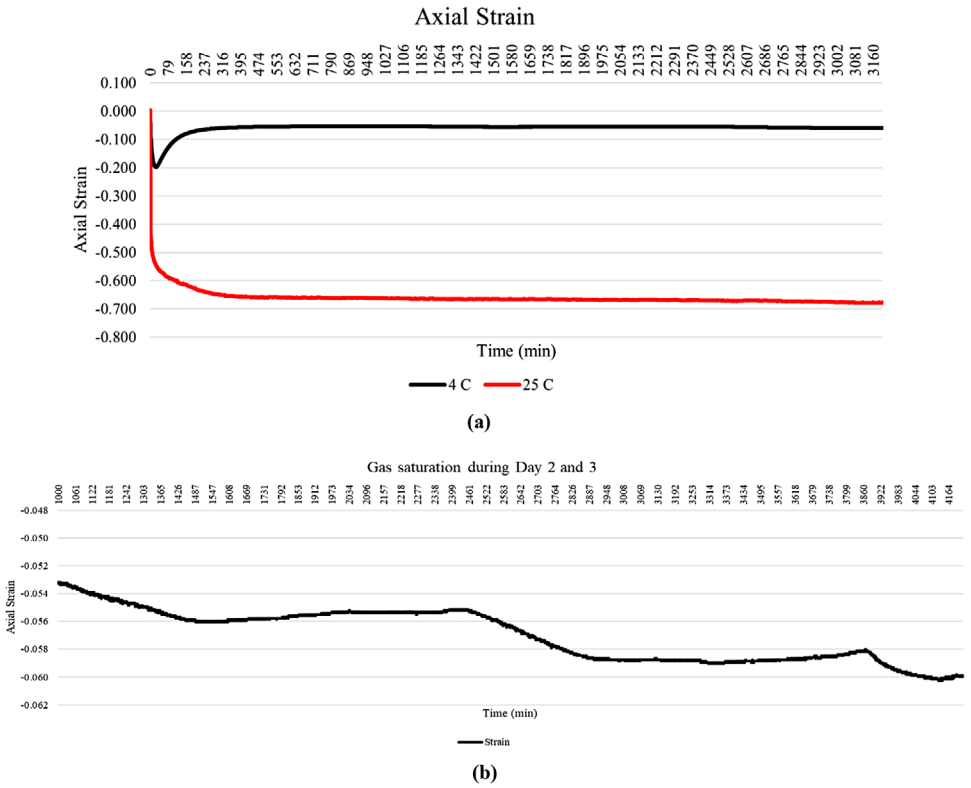

Figure 8 | (a) Comparison of axial strain changes following CO_2 adsorption at injection temperatures of 4°C and 25°C around the sample for 3200 min with an injection gas pressure of 30 bar; (b) axial strain changes in the coal sample following saturation at 4°C.

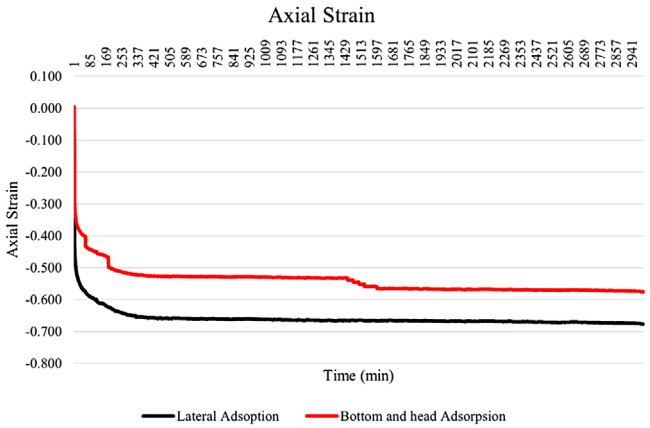

Figure 9 | Comparison of axial strain variation trends following saturation of the coal sample from the perimeter and both ends due to CO_2 adsorption at an injection pressure of 30 bar for 3000 min at 25°C.

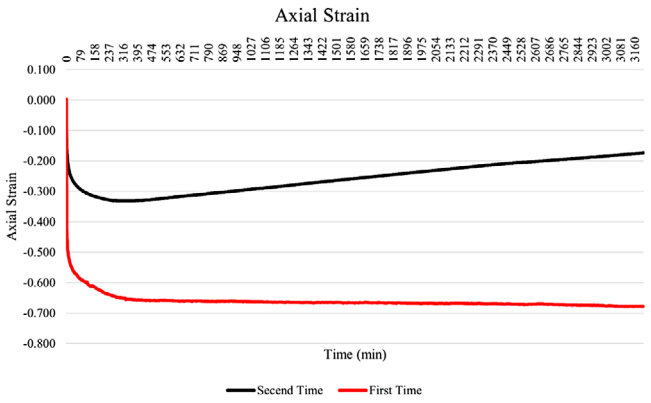

Figure 10 | Comparison of axial strain variations after re-adsorption of gas at 30-bar injection pressure following saturation with CO_2 at 25°C for 3200 min.

10 | Conclusions

ECBM is a technique used to extract methane gas from coal seams. It not only produces energy but also improves mine safety by reducing methane levels. Additionally, ECBM can be used to store CO_2 underground, mitigating greenhouse gas emissions. Iranian coal seams, with their specific characteristics, offer potential for applying these techniques. However, further research is needed to assess their feasibility in the Iranian context.

To assess the feasibility of CO_2 sequestration and ECBM in Iranian coal seams, a triaxial testing machine was developed. This machine simulates underground conditions, enabling the study of coal's behavior under these processes. It can also be used to investigate coal seams in mines and determine rock strength. Compared to other devices that are accessible worldwide, this one is extremely inexpensive to build and provides additional operating options because of its multifunctionality. Its distinct mechanical design also lowers the chance of failure by making it simple to build, fix, and maintain. It's easily repairable in case of failure.

The development of this triaxial testing apparatus represents a significant advancement in the field of coal research, particularly in the context of CO_2 sequestration and ECBM. By enabling

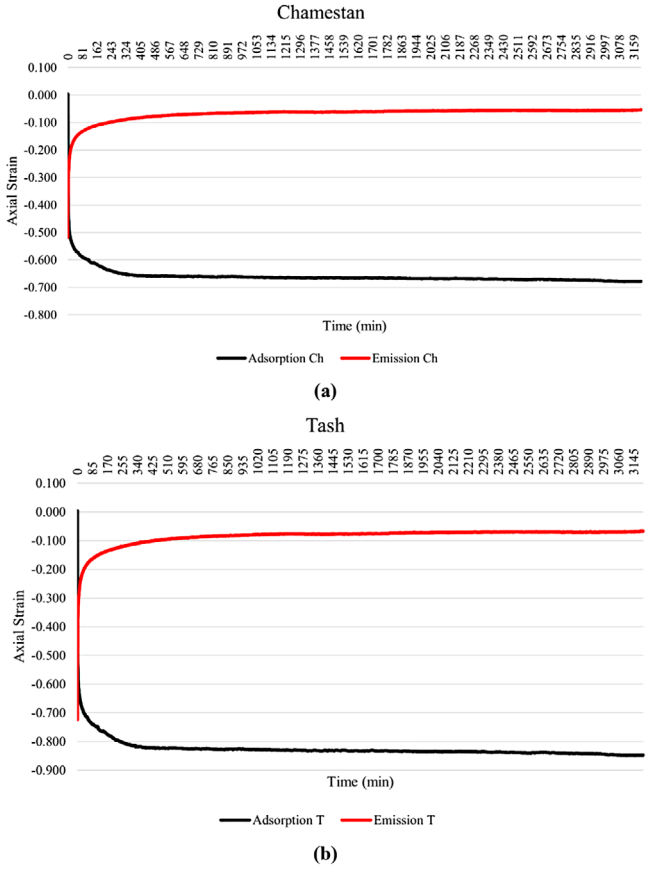

Figure 11 | (a) Comparison of the axial strain variations after CO_2 adsorption and emission from the Chamestan coal sample for 3200 min after saturation at a gas injection pressure of 30 bar; (b) comparison of the axial strain variations after CO_2 adsorption and emission from the Tash coal sample for 3200 min after saturation at a gas injection pressure of 30 bar.

precise control over experimental conditions and accurate measurement of key parameters, this apparatus provides a powerful tool for investigating the complex interactions between coal and gas. The experimental results obtained from this study have shed light on the influence of factors, such as ash content, temperature, and saturation direction, on coal's gas adsorption capacity and mechanical behavior. These findings can be utilized to optimize CO_2 sequestration and ECBM operations, leading to more efficient and sustainable energy extraction and storage practices.

For validation of the constructed device, some characteristics of coal during CO_2 adsorption were examined. On the basis of the conducted experiments, the following findings were obtained:

- A higher ash content in coal will result in a higher coal UCS. Tash's thermal coal ash concentration is around 63.29% lower than Chamestan's. For Chamestan and Tash coals, the maximum UCS calculated before failure was found to be 4.85 and 4.11 MPa, respectively.
- Coal gets more brittle as its coal ash content rises. The axial strain of Chamestan coal before uniaxial failure is around 9.17% lower than the predicted axial strain of Tash coal due to its greater ash content. For Chamestan and Tash coals, the maximum computed axial strain is equal to 0.099% and 0.109%, respectively.
- The amount of gas adsorption and the ensuing deformation decrease with increasing coal ash content. The Tash coal sample exhibits approximately 19.41% more axial strain variation and gas adsorption as a result than the Chamestan coal sample. For Tash and Chamestan coals, the estimated axial strain is 0.814% and 0.656%, respectively. Therefore, a decrease in the amount of coal ash is correlated with an increase in the gas adsorption capacity and the resulting deformation.
- The estimated axial strain following gas adsorption will drop by almost 90% when the gas is released from the Tash and Chamestan coal samples for 50 h, or the saturation time. It is possible to see that there is a 13.84% difference in the percentage change in axial strain between the Tash and Chamestan coals when comparing their axial strains. This is true even though Tash coal has a 69.23% lower ash content percentage than Chamestan coal. This reduced ash percentage suggests that Tash coal has a higher capability for gas adsorption.
- The amount of gas that coal can adsorb rises with temperature within a particular range. The strain of the coal sample at 25°C, or the axial strain variations, is almost 12.5 times more than the calculated strain at 4°C. Thus, it is evident how temperature affects the coal sample's ability to adsorb gases. The experiment's data and past research indicate that 25°C is the ideal temperature for coal to adsorb gases to the greatest extent possible.
- When the sample is saturated, the axial strain variation measured from the sample walls is about 13.72% more than the strain variation measured from the sample's ends. After the sample is saturated, the axial strain value is computed to be 0.656% and 0.555% for the sample wall and both ends, respectively. This discrepancy stems only from the fact that the gas contact surface of the coal sample is different at saturation conditions from the sample wall.
- According to the conducted studies, the amount of axial strain variations of the sample resulting from saturation under the same conditions decreased by around 70% after the sample was re-saturated. The lack of free surface in the pore walls for the reabsorption of CO_2 is the cause of this phenomenon. All of the sample's gas-accessible material is completely saturated during the first saturation, and no fresh tissue is accessible for gas adsorption during the subsequent saturation. As a result, the sample's axial strain won't be considerably altered by re-saturation.

Ethics Statement

The authors have nothing to report.

Consent

The authors have nothing to report.

Conflicts of Interest

The authors declare no conflicts of interest.

Data Availability Statement

Data will be available by request.

Endnotes

[1]Carbon dioxide.

[2]Methane.

References

1. M. Mukherjee and S. Misra, "A Review of Experimental Research on Enhanced Coal Bed Methane (ECBM) Recovery via CO_2 Sequestration," *Earth-Science Reviews* 179 (2018): 392–410.

2. Z. Kou, T. Wang, Z. Chen, and J. Jiang, " A Fast and Reliable Methodology to Evaluate Maximum CO_2 Storage Capacity of Depleted Coal Seams: A Case Study," *Energy* 231 (2021): 120992.

3. B. Lin, T. Liu, Y. Zhou, Z. Zhang, and F. Yan, "Variation of Methane Adsorption Property of Coal After the Treatment of Hydraulic Slotting and Methane Pre-Drainage: A Case Study," *Journal of Natural Gas Science and Engineering* 20 (2014): 396–406.

4. Z. Wang, X. Fu, M. Hao, et al., "Experimental Insights Into the Adsorption–Desorption of CH_4/N_2 and Induced Strain for Medium-Rank Coals," *Journal of Petroleum Science and Engineering* 204 (2021): 108705.

5. Q. Zou and B. Lin, "Fluid–Solid Coupling Characteristics of Gas-Bearing Coal Subjected to Hydraulic Slotting: An Experimental Investigation," *Energy & Fuels* 32, no. 2 (2018): 1047–1060.

6. J. W. Larsen, "The Effects of Dissolved CO_2 on Coal Structure and Properties," *International Journal of Coal Geology* 57, no. 1 (2004): 63–70.

7. C. Ö. Karacan, "Heterogeneous Sorption and Swelling in a Confined and Stressed Coal During CO_2 Injection," *Energy & Fuels* 17, no. 6 (2003): 1595–1608.

8. C. Ö. Karacan, "Swelling-Induced Volumetric Strains Internal to a Stressed Coal Associated With CO_2 Sorption," *International Journal of Coal Geology* 72, no. 3–4 (2007): 209–220.

9. F. Sereshki (2005). Improving coal mine safety by identifying factors that influence the sudden release of gases in outburst prone zones.

10. N. I. Aziz and W. Ming-Li, "The Effect of Sorbed Gas on the Strength of Coal—An Experimental Study," *Geotechnical & Geological Engineering* 17, no. 3 (1999): 387–402.

11. Q. Du, X. Liu, E. Wang, and S. Wang, "Strength Reduction of Coal Pillar After CO_2 Sequestration in Abandoned Coal Mines," *Minerals* 7, no. 2 (2017): 26.

12. Y. Ates and K. Barron, "The Effect of Gas Sorption on the Strength of Coal," *Mining Science and Technology* 6, no. 3 (1988): 291–300.

13. D. R. Viete and P. G. Ranjith, "The Effect of CO_2 on the Geomechanical and Permeability Behaviour of Brown Coal: Implications for Coal Seam CO_2 Sequestration," *International Journal of Coal Geology* 66, no. 3 (2006): 204–216.

14. E. Su, Y. Liang, Q. Zou, F. Niu, and L. Li, "Analysis of Effects of CO_2 Injection on Coalbed Permeability: Implications for Coal Seam CO_2 Sequestration," *Energy & Fuels* 33, no. 7 (2019): 6606–6615.

15. S. Zheng, Y. Yao, D. Elsworth, D. Liu, and Y. Cai, "Dynamic Fluid Interactions During CO_2-enhanced Coalbed Methane and CO_2 Sequestration in Coal Seams. Part 1: CO_2–CH_4 Interactions," *Energy & Fuels* 34, no. 7 (2020): 8274–8282.

16. K. Sampath, P. G. Ranjith, and M. S. A. Perera, "A Comprehensive Review of Structural Alterations in CO_2-interacted Coal: Insights Into CO_2 Sequestration in Coal," *Energy & Fuels* 34, no. 11 (2020): 13369–13383.

17. R. Yang, S. Liu, H. Wang, et al., "Influence of H_2O on Adsorbed CH_4 on Coal Displaced by CO_2 Injection: Implication for CO_2 Sequestration in Coal Seam With Enhanced CH_4 Recovery (CO_2-ECBM)," *Industrial & Engineering Chemistry Research* 60, no. 43 (2021): 15817–15833.

18. L. Jiang, Z. Chen, S. M. F. Ali, J. Zhang, Y. Chen, and S. Chen, "Storing Carbon Dioxide in Deep Unmineable Coal Seams for Centuries Following Underground Coal Gasification," *Journal of Cleaner Production* 378 (2022): 134565.

19. L. Sun, S. Duan, S. Zhang, W. Cheng, G. Wang, and X. Cao, "Influencing Factors and Mechanism of CO_2 Adsorption Capacity of FA-Based Carbon Sequestration Materials," *Environmental Science and Pollution Research* 30, no. 55 (2023): 117225–117237.

20. C. Zhang, E. Wang, B. Li, et al., "Laboratory Experiments of CO_2-enhanced Coalbed Methane Recovery Considering CO_2 Sequestration in a Coal Seam," *Energy* 262 (2023): 125473.

21. Q. Zou, Z. Chen, J. Zhan, et al., "Morphological Evolution and Flow Conduction Characteristics of Fracture Channels in Fractured Sandstone Under Cyclic Loading and Unloading," *International Journal of Mining Science and Technology* 33, no. 12 (2023): 1527–1540.

22. S. R. Jeong, J. H. Park, J. H. Lee, P. R. Jeon, and C.-H. Lee, "Review of the Adsorption Equilibria of CO_2, CH_4, and Their Mixture on Coals and Shales at High Pressures for Enhanced CH_4 Recovery and CO_2 Sequestration," *Fluid Phase Equilibria* 564 (2023): 113591.

23. E. F. Klitzke, F. Ketzer, M. O. Almeida, et al., "Adsorption of Methane by Modified-Biochar Aiming to Improve the Gaseous Fuels Storage/Transport Capacity: Process Evaluation and Modeling," *Environmental Science and Pollution Research* 31, no. 36 (2024): 49285–49299.

24. B. Chen, L. Fang, Z. Xu, F. M. Stuart, G. Li, and S. Xu, "Assessing the Potential for CO_2 Storage in Shallow Coal Seams Using Gas Geochemistry: A Case Study From Qinshui Basin, North China," *International Journal of Greenhouse Gas Control* 132 (2024): 104063.

25. R. Shukla, P. G. Ranjith, S. K. Choi, and A. Haque, "A Novel Testing Apparatus for Hydromechanical Investigation of Rocks: Geo-Sequestration of Carbon Dioxide," *Rock Mechanics and Rock Engineering* 45, no. 6 (2012): 1073–1085.

26. M. S. A. Perera, P. G. Ranjith, S. K. Choi, and D. Airey, "The Effects of Sub-Critical and Super-Critical Carbon Dioxide Adsorption-Induced Coal Matrix Swelling on the Permeability of Naturally Fractured Black Coal," *Energy* 36, no. 11 (2011): 6442–6450.

27. P. G. Ranjith and M. S. A. Perera, "A New Triaxial Apparatus to Study the Mechanical and Fluid Flow Aspects of Carbon Dioxide Sequestration in Geological Formations," *Fuel* 90, no. 8 (2011): 2751–2759.

28. C. Laxminarayana and P. J. Crosdale, "Role of Coal Type and Rank on Methane Sorption Characteristics of Bowen Basin, Australia Coals," *International Journal of Coal Geology* 40, no. 4 (1999): 309–325.

29. J. D. S. George and M. A. Barakat, "The Change in Effective Stress Associated With Shrinkage From Gas Desorption in Coal," *International Journal of Coal Geology* 45, no. 2–3 (2001): 105–113.

30. E. Hoek and J. A. Franklin, "Simple Triaxial Cell for Field or Laboratory Testing of Rock," *Transactions of the Institution of Mining and Metallurgy* 77 (1968): A22–A26.

31. C. R. Clarkson and R. M. Bustin, "Binary Gas Adsorption/Desorption Isotherms: Effect of Moisture and Coal Composition Upon Carbon Dioxide Selectivity Over Methane," *International Journal of Coal Geology* 42, no. 4 (2000): 241–271.

32. C. Laxminarayana and P. J. Crosdale, "Controls on Methane Sorption Capacity of Indian Coals," *AAPG Bulletin* 86, no. 2 (2002): 201–212.

33. P. Weniger, J. Franců, P. Hemza, and B. M. Krooss, "Investigations on the Methane and Carbon Dioxide Sorption Capacity of Coals From the SW Upper Silesian Coal Basin," *International Journal of Coal Geology* 93 (2012): 23–39.

34. Z. Weishauptová, O. Přibyl, I. Sýkorová, and V. Machovič, "Effect of Bituminous Coal Properties on Carbon Dioxide and Methane High Pressure Sorption," *Fuel* 139 (2015): 115–124.

35. C. R. Clarkson and R. M. Bustin, "Coalbed Methane: Current Field-Based Evaluation Methods," *SPE Reservoir Evaluation & Engineering* 14, no. 01 (2011): 60–75.

36. P. Dutta, S. Bhowmik, and S. Das, "Methane and Carbon Dioxide Sorption on a Set of Coals From India," *International Journal of Coal Geology* 85, no. 3–4 (2011): 289–299.

37. M. Faiz, A. Saghafi, N. Sherwood, and I. Wang, "The Influence of Petrological Properties and Burial History on Coal Seam Methane Reservoir Characterisation," *International Journal of Coal Geology* 70, no. 1–3 (2007): 193–208.

38. V. N. Romanov, T.-B. Hur, J. J. Fazio, B. H. Howard, and G. A. Irdi, "Comparison of High-Pressure CO_2 Sorption Isotherms on Central Appalachian and San Juan Basin Coals," *International Journal of Coal Geology* 118 (2013): 89–94.

39. P. Weniger, W. Kalkreuth, A. Busch, and B. M. Krooss, "High-pressure Methane and Carbon Dioxide Sorption on Coal and Shale Samples From the Paraná Basin, Brazil," *International Journal of Coal Geology* 84, no. 3–4 (2010): 190–205.

40. V. S. Vutukuri and K. Katsuyama (1994). Introduction to rock mechanics. *(No Title)*.

41. S. Day, R. Sakurovs, and S. Weir, "Supercritical Gas Sorption on Moist Coals," *International Journal of Coal Geology* 74, no. 3–4 (2008): 203–214.

42. S. Day, R. Fry, and R. Sakurovs, "Swelling of Australian Coals in Supercritical CO_2," *International Journal of Coal Geology* 74, no. 1 (2008): 41–52.

43. S. Day, R. Fry, and R. Sakurovs, "Swelling of Coal in Carbon Dioxide, Methane and Their Mixtures," *International Journal of Coal Geology* 93 (2012): 40–48.

44. S. Day, R. Fry, R. Sakurovs, and S. Weir, "Swelling of Coals by Supercritical Gases and Its Relationship to Sorption," *Energy & Fuels* 24, no. 4 (2010): 2777–2783.